ENGINEERING TRANSACTIONS • *Engng. Trans.* • **45**, 3–4, 375–394, 1997
Polish Academy of Sciences • Institute of Fundamental Technological Research

NUMERICAL SIMULATION OF MASONRY PANELS

N.M. AUCIELLO (POTENZA) and A. ERCOLANO (CASSINO)

In the present paper, a new linear complementary formulation for contact problems under Coulomb law of friction (which takes into consideration the rigid body modes) is presented. Moreover, a finite element model for the numerical simulation of masonry panels is developed and a technique for fast updating of the interface elements is reported. The masonry is considered as a composite material produced by the inclusion of bricks into the matrix of mortar. The two components are supposed to be perfectly linear elastic, the unilateral contact being restricted to the blocks-mortar interfaces. An example of masonry panel is reported.

1. INTRODUCTION

Structural models for masonry have been widely proposed and discussed in recent years. Most of the research has been carried out by investigators of such countries like Italy for example, where due to the huge architectural heritage, both the design techniques and consolidation techniques are strongly needed. Depending essentially on the ratio between the size of the single block and the size of the whole structure, two different approaches can be recognized. If each unit or block, very often a natural stone, has relatively consistent dimensions, the structural behaviour is strongly affected by the exact position and shape of every single block rather than by their constitutive parameters. This kind of masonry structures has been called monumental or block structures. Unfortunately, in this case, in order to obtain exact information on the stress field and fracture lines, an accurate discretization, pratically a stone-by-stone discretization, must be adopted. On the other hand, there are structures where, due to the small size of single units with respect to the whole structure, a regular texture is recognisable. In this case masonry can be viewed as a continuum, more properly as a composite, where the mortar is the matrix and the units, usually bricks, represent the inclusions. The first approach, the discrete block model, was introduced in the sixties by HEYMAN [15] in connection with the limit analysis for block-arches. Further contributions to the discrete model came more than a decade later (LIVESLEY [18], FRANCIOSI [13]). Starting from the eighties, both

the analytical approach (DEL PIERO [9]) and the numerical approach (ISHIYAMA [16], BLASI, SPINELLI [3], CHAUDHARY and BATHE [4], YIM, CHOPRA and PENZIEN [28], ERCOLANO [11, 12]), have been extensively applied to these structures.

The first analytical formulation within a convex analysis frame of a continuum model for masonry was developed by two researchers: G. ROMANO and M. ROMANO [25]. This new continuum, the no-tension or masonry-like material, called N.R.T. model (not resisting tension model), is postulated by the absence of tensile stress in the whole domain and normality assumption between the stress field and the inelastic deformation field rule. Some years later, other fundamental results were obtained (GIAQUINTA and GIUSTI [14], DEL PIERO [6, 7]).

As a general feature, the papers dealing with block models, because of the numerical difficulties arising in case of contact problems and geometrical nonlinearities, are generally concerned with structures of a few blocks as trilites, arches or columns. On the continuum side, the original N.R.T. model seems to be not able to deal with the texture of the masonry and the existence of the mortar.

To overcome these limitations, some authors have followed a micromechanical approach considering the masonry as a composite (PANDE, LIANG and MIDDLETON [23], PIETRUSZCZAK and NIU [24], ANTHOINE [2], LUCIANO and SACCO [19]), but the nonlinear behaviour is still far from being defined. At this stage of the knowledge it is clear that the different approaches in the field, theoretical, numerical and experimental, must proceed together with a deep communication exchange. Indeed, numerical and experimental analysis are the only tools that provide insight into the structural behaviour and can validate the theory. Anyway, numerical simulation still remains to be the only way to analyse complex shapes under complex loads.

In the paper, both units and mortar are discretized via the finite element technique under the following assumptions:

- infinitesimal displacement field,
- perfectly linear elasticity of both units (brick or block) and mortar (head and bed joint),
- Coulomb friction law between the units and mortar.

In the literature, contact problems can be either reduced to a linear complementarity problem, the L.C.P. for short (KLARBRING [21]), or solved using the penalty methods or Lagrangian multipliers methods (KIKUCHI, ODEN [20]). A method which is somewhere between the last two and seems to take the best of both methods, is the augmented Lagrangian method, A.L.M. The A.L.M. appeared (see KLARBRING [22]) in several papers in a short period of time (ALART, CURNIER [1], DE SAXCE, FENG [10], SIMO, LAURSEN [26]) and has become the natural competitor of the L.C.P. methods. In the paper both approaches are presented and then discussed through the analysis of some masonry panels.

The contributions of the paper in this field are basically two: a new linear complementary formulation and a finite element formulation for mortar films. The first result is a generalization, under the Coulomb law of friction, of a method presented by DEL PIERO [8]. The friction conditions are imposed in the fashion proposed by LEE [17]. The second one is a finite element model which simulates the mortar films. Further a numerical technique for fast updating of the stiffness matrices of the interface elements is used. The procedure is based on the transformation matrices, which change the nodal coordinates.

• Obviously, for high value of the friction angle, contact condition can occur only under sticking condition, so that the problem, although still path-dependent, becomes non-dissipative and turns out to be more similar to the no-tensile stress assumption of the masonry-like material: $\mathbf{t}_n \cdot \mathbf{n} \geq 0$, $\forall \mathbf{n}$ on Ω is replaced by: $\mathbf{t}_n \cdot \mathbf{n} \geq 0$, $\forall \mathbf{n}$ on $\partial\Omega^C$, where $\partial\Omega^C$ is the contact area and therefore the set of all the bricks-mortar interfaces.

2. SETTING OF THE PROBLEM

The masonry panel is assumed to present a texture produced by the regular repetition of units (bricks or blocks), with or without the mortar interposition, as shown in Fig. 1.

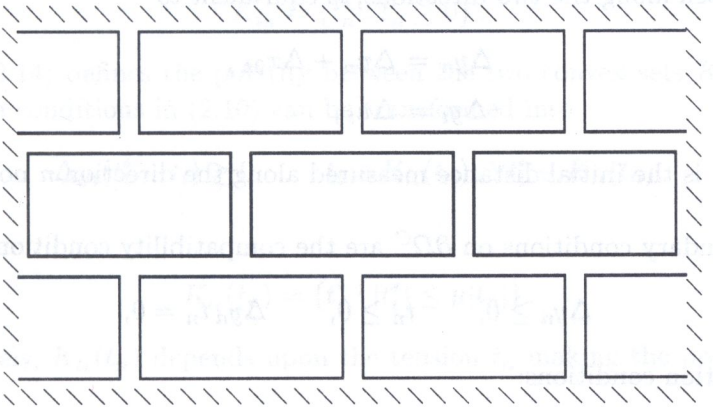

FIG. 1. The model

The well known field equations in Ω, the compatibility, the constitutive and the equilibrium equations are

$$\mathbf{D}\,\mathbf{u} = \boldsymbol{\varepsilon}, \tag{2.1}$$

$$\mathbf{C}\,\boldsymbol{\varepsilon} = \boldsymbol{\sigma}, \tag{2.2}$$

$$\operatorname{div}\mathbf{T} + \mathbf{b} = \mathbf{0}. \tag{2.3}$$

The standard boundary conditions are:

$$\mathbf{u} = \overline{\mathbf{u}} \qquad \text{on} \quad \partial\Omega^{\overline{\mathbf{u}}}, \tag{2.4}$$

$$\mathbf{t}_n = \overline{\mathbf{t}}_n \qquad \text{on} \quad \partial\Omega^{\overline{\mathbf{t}}_n}. \tag{2.5}$$

The discontinuities in these fields are assumed to appear only in some area, namely $\partial\Omega^C$, which collects all the interfaces between the bricks or the brick-mortar interfaces, if mortar is supposed to exist. In other words, $\partial\Omega^C$ is a geometrical surface made by all those areas which are common boundaries of elementary bodies. Obviously the three different areas must be distinct: i.e. $\partial\Omega^{\overline{\mathbf{u}}} \cap \partial\Omega^{\overline{\mathbf{t}}_n} = \partial\Omega^{\overline{\mathbf{u}}} \cap \partial\Omega^C = \partial\Omega^{\overline{\mathbf{t}}_n} \cap \partial\Omega^C = \emptyset$. The actual relative displacement $\Delta\mathbf{u} = (\Delta u_n, \Delta u_t)^t$ among the two generic surfaces, say $\partial\Omega_a^C$, $\partial\Omega_b^C$ in contact, expressed in the local frame n, t, is given by

$$\begin{aligned} \Delta u_n &= u_{bn} - u_{an}\,, \\ \Delta u_t &= u_{bt} - u_{at}\,. \end{aligned} \tag{2.6}$$

The actual relative distance $\boldsymbol{\Delta}\mathbf{y}$ between these surfaces is given by

$$\mathbf{x}_{0a} + \mathbf{u}_a + \boldsymbol{\Delta}\mathbf{y} = \mathbf{x}_{0b} + \mathbf{u}_b \tag{2.7}$$

which, written along the two directions, is equivalent to

$$\begin{aligned} \Delta y_n &= \Delta u_n + \Delta x_{0n}\,, \\ \Delta y_t &= \Delta u_t\,, \end{aligned} \tag{2.8}$$

where Δx_{0n} is the initial distance measured along the direction n normal to the surface.

The boundary conditions on $\partial\Omega^C$ are the compatibility conditions:

$$\Delta y_n \geq 0, \qquad t_n \geq 0, \qquad \Delta y_n\, t_n = 0, \tag{2.9}$$

and the friction conditions:

$$\begin{aligned} &-\mu t_n \leq t_t \leq \mu t_n\,, \\ &\Delta y_t = 0 \quad \text{if} \quad -\mu t_n < t_t < \mu t_n\,, \\ &\Delta y_t \geq 0 \quad \text{if} \quad t_t = \mu t_n\,, \\ &\Delta y_t \leq 0 \quad \text{if} \quad t_t = -\mu t_n\,. \end{aligned} \tag{2.10}$$

For an easier understanding in (2.10), the static frictional contact conditions have been assumed. To obtain the quasi-static frictional contact conditions, valid for

the p-th time interval $\Delta t_p = [t_{p+1} - t_p]$, it is sufficient to replace the displacement Δy_t in (2.10) with its time variation:

$$\left[\Delta \dot{y}_{t_p}\right] \simeq [\Delta y_{t_{p+1}} - \Delta y_{t_p}]/\Delta t_p \,.$$

The corresponding energy loss is given by:

$$t_t[\Delta y_{t_{p+1}} - \Delta y_{t_p}] \geq 0.$$

The fields of both the admissible displacements and admissible tensions satisfying the normal conditions are

$$K_n^T = \mathbf{t}_n \in \mathbf{U}_{\partial\Omega^C}^{n'} \,:\, \mathbf{t}_n \cdot n = t_n \geq 0 \qquad \text{on} \quad \partial\Omega^C, \tag{2.12}$$

$$K_n^U = \mathbf{u} \in \mathbf{U} \,:\, \Delta\mathbf{u} \cdot \mathbf{n} + \Delta x_{0n} \geq 0 \qquad \text{on} \quad \partial\Omega^C, \tag{2.13}$$

where the field displacement $\mathbf{U}$ satisfies the relative boundary condition in (2.4), and $U_{\partial\Omega^C}^{n'}$ is the dual space of displacement on $\partial\Omega^C$.

The normal contact condition in (2.9) (KLARBRING [21]) is equivalent to

$$\Delta y_n(t_n^* - t_n) \geq 0, \qquad t_n \in K_{t_n},\ \forall t_n^* \in K_{t_n}\,, \tag{2.14}$$

where

$$K_{t_n} = \{t_n^* : t_n^* \geq 0\}\,. \tag{2.15}$$

Equation (2.14) defines the polarity between the two convex sets K_n^U and K_n^T. The friction conditions in (2.10) can be transformed into

$$\Delta y_t(t_t^* - t_t) \geq 0, \qquad t_t \in K_{t_t}(t_n),\ \forall t_t^* \in K_{t_t}(t_n), \tag{2.16}$$

where

$$K_{t_t}(t_n) = \{t_t^* : |t_t^*| \leq \mu |t_n|\}\,. \tag{2.17}$$

Unfortunately, $K_{t_t}(t_n)$ depends upon the tension t_n making the problem path-dependent.

3. FINITE ELEMENT FORMULATION

The weak form of the problem can be set as follows:

$$\int_\Omega \boldsymbol{\sigma}(\mathbf{u}) \cdot \boldsymbol{\varepsilon}(\mathbf{u}^*) = \int_{\partial\Omega^C} t_{nt} \Delta u_t^* + \int_{\partial\Omega^C} t_{nn} \Delta u_n^* + \int_\Omega \mathbf{b} \cdot \mathbf{u}^* + \int_{\partial\Omega^{\bar{\mathbf{t}}_n}} \bar{\mathbf{t}}_n \cdot \mathbf{u}^*, \quad \forall \mathbf{u}^* \in \mathbf{U}. \tag{3.1}$$

By means of a Galerkin projection, Eq. (3.1) becomes

$$\mathbf{K}\,\mathbf{u} + \mathbf{C}_n^T \mathbf{t}_n + \mathbf{C}_t^T \mathbf{t}_t + \mathbf{f} = \mathbf{0}. \tag{3.2}$$

The discretized versions of (2.10) and (2.9) are

$$\begin{gathered} \mathbf{C}_n + \Delta\mathbf{y}_n = \Delta\mathbf{x}_o\,, \\ \Delta\mathbf{y}_n \geq \mathbf{0}, \qquad \mathbf{t}_n \geq \mathbf{0}, \qquad \mathbf{t}_n \cdot \Delta\mathbf{y}_n = \mathbf{0}, \end{gathered} \tag{3.3}$$

and

$$\begin{aligned} &-\mu\mathbf{t}_n \leq \mathbf{t}_t \leq \mu\mathbf{t}_n\,, \\ &\Delta\mathbf{y}_t = \mathbf{0} \quad \text{if} \quad -\mu\mathbf{t}_n < \mathbf{t}_t < \mu\mathbf{t}_n\,, \\ &\Delta\mathbf{y}_t \geq \mathbf{0} \quad \text{if} \quad \mathbf{t}_t = \mu\mathbf{t}_n\,, \\ &\Delta\mathbf{y}_t \leq \mathbf{0} \quad \text{if} \quad \mathbf{t}_t = -\mu\mathbf{t}_n\,, \end{aligned} \tag{3.4}$$

where

$$\begin{aligned} \Delta\mathbf{y}_n &= [\mathbf{u}_{bn} - \mathbf{u}_{an}] + \Delta\mathbf{x}_{on} = \mathbf{C}_n\mathbf{u} + \Delta\mathbf{x}_{on}\,, \\ \Delta\mathbf{y}_t &= [\mathbf{u}_{bt} - \mathbf{u}_{at}] = \Delta\mathbf{u}_t = \mathbf{C}_t\mathbf{u}\,. \end{aligned} \tag{3.5}$$

In (3.5) vectors $\mathbf{u}_b = (\mathbf{u}_{bn}, \mathbf{u}_{bt})^t$ and $\mathbf{u}_a = (\mathbf{u}_{an}, \mathbf{u}_{at})^t$ collect the displacements of all the pairs of nodes which may be in contact. It is further supposed that the nodal displacements have been chosen according to the local frames (n, t) at the boundary, with n normal to the unilateral contact area.

Introducing the two variables $\Delta\mathbf{t}_t^-$ and $\Delta\mathbf{t}_t^+$, the inequalities in (3.4) can be reduced to

$$\begin{aligned} \Delta\mathbf{t}_t^- &= \mu\mathbf{t}_n - \mathbf{t}_t\,, \\ \Delta\mathbf{t}_t^+ &= \mu\mathbf{t}_n + \mathbf{t}_t\,. \end{aligned} \tag{3.6}$$

Finally, all the constraints in (3.3) and (3.4) can be set in the form

$$\begin{aligned} &\mathbf{t}_n \geq \mathbf{0}, \quad \Delta\mathbf{y}_n \geq \mathbf{0}, \quad \mathbf{t}_n \cdot \Delta\mathbf{y}_n = \mathbf{0}, \\ &\Delta\mathbf{t}_t^+ \geq \mathbf{0}, \quad \Delta\mathbf{y}_t^+ \geq \mathbf{0}, \quad \Delta\mathbf{y}_t^+ \cdot \Delta\mathbf{t}_t^+ = \mathbf{0}, \\ &\Delta\mathbf{t}_t^- \geq \mathbf{0}, \quad \Delta\mathbf{y}_t^- \geq \mathbf{0}, \quad \Delta\mathbf{y}_t^- \cdot \Delta\mathbf{t}_t^- = \mathbf{0}, \end{aligned} \tag{3.7}$$

where

$$[\Delta\mathbf{y}_t]^+ = \frac{1}{2}\left[|\Delta\mathbf{y}_t| + \Delta\mathbf{y}_t\right] \qquad \text{and} \qquad [\Delta\mathbf{y}_t]^- = \frac{1}{2}\left[|\Delta\mathbf{y}_t| - \Delta\mathbf{y}_t\right]$$

are the two projections of $\Delta\mathbf{y}_t$:

$$\Delta\mathbf{y}_t = [\Delta\mathbf{y}_t]^+ - [\Delta\mathbf{y}_t]^-. \tag{3.8}$$

From the equalities in (3.6), the values of the tensions can be obtained

$$\begin{aligned} \mathbf{t}_t &= \left(-\Delta\mathbf{t}_t^- + \Delta\mathbf{t}_t^+\right)/2, \\ \mathbf{t}_n &= \left(\Delta\mathbf{t}_t^- + \Delta\mathbf{t}_t^+\right)/(2\mu). \end{aligned} \tag{3.9}$$

3.1. Augmented Lagrangian method

Following the approach given in (KLARBRING [22]), the constraints (3.3) or $(3.7)_1$ are equivalent to the inequality

$$(-\mathbf{C}_n\mathbf{u} + \Delta\mathbf{x}_{0n})\,(\mathbf{t}_n^* - \mathbf{t}_n) \geq 0, \qquad \mathbf{t}_n \in \mathbf{K}_{t_n},\ \forall \mathbf{t}_n^* \in \mathbf{K}_{t_n}, \tag{3.10}$$

where $\mathbf{K}_{t_n} = \{\mathbf{t}_n^* : \mathbf{t}_n^* \geq 0\}$. Equation (3.10) can be obviously rewritten as

$$\{\mathbf{t}_n - [\mathbf{t}_n - \varrho_n(-\mathbf{C}_n\mathbf{u} + \Delta\mathbf{x}_{0n})]\}\,(\mathbf{t}_n^* - \mathbf{t}_n) \geq 0, \tag{3.11}$$
$$\mathbf{t}_n \in \mathbf{K}_{t_n},\ \forall \mathbf{t}_n^* \in \mathbf{K}_{t_n},\quad \varrho_n \in R^+.$$

Condition (3.11) means that $\mathbf{t}_n$ is the projection of $[\mathbf{t}_n - \varrho_n(-\mathbf{C}_n\mathbf{u} + \Delta\mathbf{x}_{0n})]$ onto the cone $\mathbf{K}_{t_n}$, i.e.

$$\mathbf{t}_n = [\mathbf{t}_n - \varrho_n(-\mathbf{C}_n\mathbf{u} + \Delta\mathbf{x}_{0n})]_{K_n^T} = [\mathbf{t}_n + \varrho_n(\mathbf{C}_n\mathbf{u} - \Delta\mathbf{x}_{0n})]^+ . \tag{3.12}$$

In the same fashion, the other two sets of conditions $(3.7)_2$, $(3.7)_3$, lead to

$$\begin{aligned} \Delta\mathbf{t}_t^+ &= \left[\Delta\mathbf{t}_t^+ - \varrho_t\Delta\mathbf{y}_t^+\right]^+, \\ \Delta\mathbf{t}_t^- &= \left[\Delta\mathbf{t}_t^- - \varrho_t\Delta\mathbf{y}_t^-\right]^+. \end{aligned} \tag{3.13}$$

Now the solution set can be obtained by iterative solution of the equilibrium equation

$$\mathbf{K}\mathbf{u}_p + \mathbf{C}_n^T\mathbf{t}_{n_p} + \mathbf{C}_t^T\mathbf{t}_{t_p} + \mathbf{f} = \mathbf{0} \tag{3.14}$$

where, at each p-th step, tensions are updated by means of

$$\begin{aligned} \mathbf{t}_{n_{p+1}} &= [\mathbf{t}_{n_p} + \varrho_n(\mathbf{C}_n\mathbf{u}_p - \boldsymbol{\Delta}\mathbf{x}_{0n})]^+, \\ \Delta\mathbf{t}_{t_{p+1}}^+ &= \left[\mu\mathbf{t}_{n_p} + \mathbf{t}_{t_p} - \varrho_t\Delta\mathbf{y}_t^+\right]^+, \\ \Delta\mathbf{t}_{t_{p+1}}^- &= \left[\mu\mathbf{t}_{n_p} - \mathbf{t}_{t_p} - \varrho_t\Delta\mathbf{y}_t^-\right]^+, \\ \mathbf{t}_{t_{p+1}} &= \left[-\Delta\mathbf{t}_{t_{p+1}}^- + \Delta\mathbf{t}_{t_{p+1}}^+\right]/2. \end{aligned} \tag{3.15}$$

When mortar films are supposed to exist between the bricks and they are discretized by a particular finite element, a gap or interface element, compatibility conditions (3.3) are automatically satisfied when the stiffness matrices of the interface elements are updated. The elements, in this case, play the role of a finite penalty function. Equation (3.14) becomes

$$\mathbf{K}_p\mathbf{u}_p + \mathbf{C}_t^T\mathbf{t}_{t_p} + \mathbf{f} = \mathbf{0}. \tag{3.16}$$

In (3.16) the stiffness matrix is made of two parts

$$\mathbf{K}_p = \mathbf{K}_b + \mathbf{K}_{pf}\,, \tag{3.17}$$

$\mathbf{K}_b$ being the global brick stiffness matrix and $\mathbf{K}_{pf}$ – the global stiffness matrix referred to those mortar films where, in the p-th iteration, the contact has occurred. For the friction condition, still an A.L.M. method can be applied.

3.2. The linear complementary problem LCP

It is well known (KLARBRING [21]) that the contact problem set by Eqs. (3.2), (3.3) and (3.4), if $\mathbf{K}$ is positive definite, can be reduced to a linear complementary problem. For $\mathbf{K}$ positive semidefinite, under the assumption of prescribed tangential tensions, a method which reduces the problem to a L.C.P. has been presented (STAVROULAKIS, PANAGIOTOPOULOS, AL-FAHED [27]). Successively (LEE [17]) the same approach has been generalized to the case of Coulomb friction. In both the papers, a local frame is considered for each free body so that any absolute node displacement is obtained by adding a rigid body motion to the relative displacement. As a counterpart, for each body, equilibrium equations must be considered. Because every equation can be seen as a couple of inequalities, the problem can still be included in an L.C.P. frame by means of decomposition of every rigid body displacement component into its positive and negative part. Obviously the price to be paid is a growth in the size of the problem. In a plane, for every rigid body motion allowed, six couples of unknown parameters must be introduced. In (DEL PIERO [8]), in the frictionless case, a much more effective force-based method has been presented. In the present paper, following this force-based approach, Coulomb friction will be included. No local frames are introduced so that the L.C.P. reduction generally saves six couples of unknowns for each free body included in the structure.

It is supposed that the discretized contact conditions are given through m couples of nodes. In other words, the contact problem depends upon the definition of two couples of vectors $\mathbf{t}_n$, $\boldsymbol{\Delta}\mathbf{y}_n$ and $\mathbf{t}_t$, $\boldsymbol{\Delta}\mathbf{y}_t$ which describe tensions and relative distances on the contact surface. Tensions have to be in equilibrium with the applied loads $\mathbf{b}_{0n}$ and $\mathbf{b}_{0t}$. Without any loss of generality, a rigid body configuration of the structure is supposed to be defined by i parameters, for instance the last i: Δy_n^{m-i+1}, Δy_n^{m-i}, ..., Δy_n^m, which are involved in the normal compatibility conditions. Here $i = 3 \times r$, where r is the number of free bodies. Then all the previous four vectors can be decomposed into two subvectors. For example, the vector $\boldsymbol{\Delta}\mathbf{y}_n$ can be decomposed into $\boldsymbol{\Delta}\mathbf{y}_n^{m-i}$ and $\boldsymbol{\Delta}\mathbf{y}_n^i$. At this stage, applying the force-based method, the final configuration can be thought as a rigid body motion defined by $\boldsymbol{\Delta}\mathbf{y}_n^i$ plus an elastic deformation caused by the loads $\mathbf{t}_n^{m-i}$, $\mathbf{t}_t^m$, $\mathbf{b}_{0n}$ and $\mathbf{b}_{0t}$, $\mathbf{t}_n^i$ being the dual variables of $\boldsymbol{\Delta}\mathbf{y}_n^i$ obtained by equilibrium equations

$$\mathbf{R}_n \mathbf{t}_n^{m-i} + \mathbf{R}_t \mathbf{t}_t^m + \mathbf{t}_{n0}^i = \mathbf{t}_n^i \,. \tag{3.18}$$

The explicit forms of the generic constraints in (3.5) are:

$$\begin{aligned} \mathbf{x}_{0na}^{m-i} + \mathbf{u}_{ena}^{m-i} + \mathbf{u}_{Rna}^{m-i} + \mathbf{u}_{0na}^{m-i} + \boldsymbol{\Delta}\mathbf{y}_n^{m-i} &= \mathbf{x}_{0nb}^{m-i} + \mathbf{u}_{enb}^{m-i} + \mathbf{u}_{Rnb}^{m-i} + \mathbf{u}_{0nb}^{m-i} \,, \\ \mathbf{u}_{eta}^m + \mathbf{u}_{Rta}^m + \mathbf{u}_{0ta}^m + \boldsymbol{\Delta}\mathbf{y}_t^m &= \mathbf{u}_{etb}^m + \mathbf{u}_{Rtb}^m + \mathbf{u}_{0tb}^m \,, \end{aligned} \tag{3.19}$$

which can be rewritten as

$$\begin{aligned} \Delta\mathbf{y}_n^{m-i} &= \Delta\mathbf{x}_{0n}^{m-i} + \Delta\mathbf{u}_{en}^{m-i} + \Delta\mathbf{u}_{Rn}^{m-i} + \Delta\mathbf{u}_{0n}^{m-i}, \\ \Delta\mathbf{y}_t^m &= \Delta\mathbf{u}_{et}^m + \Delta\mathbf{u}_{Rt}^m + \Delta\mathbf{u}_{0t}^m. \end{aligned} \tag{3.20}$$

The last i compatibility conditions are left in the form

$$\Delta\mathbf{u}_n^i = \Delta\mathbf{y}_n^i - \Delta\mathbf{x}_{0n}^i. \tag{3.21}$$

Here $\Delta\mathbf{x}_{0n}^{m-i}$ is the relative initial gap, $\Delta\mathbf{u}_{en}^{m-i}$ and $\Delta\mathbf{u}_{et}^m$ denote the elastic relative displacements caused by the unknown vectors $\mathbf{t}_n^{m-i}$ and $\mathbf{t}_t^m$, $\Delta\mathbf{u}_{Rn}^{m-i}$ and $\Delta\mathbf{u}_{Rt}^m$ are the relative rigid body displacements caused by $\Delta\mathbf{u}_n^i$. Finally, $\Delta\mathbf{u}_{0n}^{m-i}$ and $\Delta\mathbf{u}_{0t}^m$ represent the elastic relative displacements caused by the loads $\mathbf{b}_{0n}$ and $\mathbf{b}_{0t}$.

At the end, the $(m-i)$ compatibility equations along n and the m compatibility equations along n can be written in the form

$$\begin{aligned} \mathbf{A}_{n,n}\,\mathbf{t}_n^{m-i} + \mathbf{A}_{n,t}\,\mathbf{t}_t^m - \mathbf{R}_n^T\Delta\mathbf{u}_n^i + \Delta\mathbf{u}_{no}^{m-i} + \Delta\mathbf{y}_n^{m-i} &= \Delta\mathbf{x}_o^{m-i}, \\ \mathbf{A}_{t,n}\,\mathbf{t}_n^{m-i} + \mathbf{A}_{t,t}\,\mathbf{t}_t^m - \mathbf{R}_t^T\Delta\mathbf{u}_n^i + \Delta\mathbf{u}_{to}^{m-i} + \Delta\mathbf{y}_t^m &= \Delta\mathbf{x}_o^{m-i}. \end{aligned} \tag{3.22}$$

Subtituiting from (3.21) the value of $\Delta\mathbf{u}_n^i$, Eq. (3.22) becomes

$$\begin{aligned} \mathbf{A}_{n,n}\,\mathbf{t}_n^{m-i} + \mathbf{A}_{n,t}\,\mathbf{t}_t^m - \mathbf{R}_n^T\Delta\mathbf{y}_n^i + \Delta\mathbf{u}_{no}^{m-i} + \Delta\mathbf{y}_n^{m-i} &= \Delta\mathbf{x}_o^{m-i} + \mathbf{R}_n^T\Delta\mathbf{x}_{0n}^i, \\ \mathbf{A}_{t,n}\,\mathbf{t}_n^{m-i} + \mathbf{A}_{t,t}\,\mathbf{t}_t^m - \mathbf{R}_t^T\Delta\mathbf{y}_n^i + \Delta\mathbf{u}_{to}^{m-i} + \Delta\mathbf{y}_t^m &= \Delta\mathbf{x}_o^{m-i} + \mathbf{R}_t^T\Delta\mathbf{x}_{0n}^i. \end{aligned} \tag{3.23}$$

Equation $(3.9)_2$ can also be written in the forms

$$2\mu\mathbf{I}_E\,\mathbf{t}_n^{m-i} + 2\mu\mathbf{I}_R\,\mathbf{t}_n^I + \Delta\mathbf{t}_{t1}^+ + \Delta\mathbf{t}_{t1}^- = 0, \tag{3.24}$$

where

$$\mathbf{I}_E = \begin{bmatrix} \mathbf{I}_{(m-i,m-i)} \\ \mathbf{0}_{(i,m-i)} \end{bmatrix}, \qquad \mathbf{I}_R = \begin{bmatrix} \mathbf{0}_{(m-i,i)} \\ \mathbf{I}_{(i,i)} \end{bmatrix}. \tag{3.25}$$

The system of the equations (3.23), (3.18) and (3.24), with the substitution $\mathbf{t}_t^m = (-\Delta\mathbf{t}_t^- + \Delta\mathbf{t}_t^+)/2$, can be written in the following matrix form:

$$\begin{bmatrix} \mathbf{A}_{n,n} & \mathbf{0} & \mathbf{A}_{n,t}/2 & -\mathbf{A}_{n,t}/2 \\ -\mathbf{R}_n & \mathbf{I} & -\mathbf{R}_t/2 & \mathbf{R}_t/2 \\ \mathbf{A}_{t,n} & \mathbf{0} & \mathbf{A}_{t,t}/2 & -\mathbf{A}_{t,t}/2 \\ 2\mu\mathbf{I} & 2\mu\mathbf{I} & \mathbf{I} & -\mathbf{I} \end{bmatrix} \begin{vmatrix} \mathbf{t}_n^{m-i} \\ \mathbf{t}_n^I \\ \Delta\mathbf{t}_{t1}^+ \\ \Delta\mathbf{t}_{t1}^- \end{vmatrix} + \begin{bmatrix} \mathbf{I} & -\mathbf{R}_n^T & \mathbf{0} & \mathbf{0} \\ \mathbf{0} & \mathbf{0} & \mathbf{0} & \mathbf{0} \\ \mathbf{0} & -\mathbf{R}_t^T & \mathbf{I} & -\mathbf{I} \\ \mathbf{0} & \mathbf{0} & \mathbf{0} & \mathbf{0} \end{bmatrix} \begin{vmatrix} \Delta\mathbf{y}_n^{m-i} \\ \Delta\mathbf{y}_n^i \\ \Delta\mathbf{y}_t^+ \\ \Delta\mathbf{y}_t^- \end{vmatrix} = \begin{vmatrix} \Delta\mathbf{x}_0^{m-i} - \Delta\mathbf{u}_{n_0}^{m-i} + \mathbf{R}_n^T\Delta\mathbf{x}_{0n}^i \\ \mathbf{t}_{n0}^i \\ -\Delta\mathbf{u}_{t_0}^m + \mathbf{R}_t^T\Delta\mathbf{x}_{0n}^i \\ \mathbf{0} \end{vmatrix}. \tag{3.26}$$

Equations (3.26) and (3.7), after obvious transformations, give rise to the following general linear complementarity problem

$$\mathbf{A}\,\mathbf{t} + \mathbf{B}\,\boldsymbol{\Delta}\mathbf{y} = \mathbf{c}_o\,,$$

$$\mathbf{t} \geq \mathbf{0}, \qquad \boldsymbol{\Delta}\mathbf{y} \geq \mathbf{0}, \qquad \mathbf{t} \cdot \boldsymbol{\Delta}\mathbf{y} = \mathbf{0}. \tag{3.27}$$

Equation (3.27) is called general because for the standard linear complementarity problem we have $\mathbf{B} = \mathbf{I}$, $\mathbf{I}$ being the identity matrix. Anyway, this problem can be solved by the Lemke bimatrix method, (STAVROULAKIS, PANAGIOTOPOULOS, AL-FAHED [27], COTTLE, PANG, STONE [5], LEE [17]). The well-posedness of the problem is similar to the frictionless case which has been discussed in (DEL PIERO [8]). A sufficient condition for a unique solution is the existence of a positive linear combination of the tensions $\mathbf{t}_n^{m-i}$ and $\mathbf{t}_n^i$ which satisfy (3.18) with $\mathbf{t}_t^m = \mathbf{0}$.

3.3. The interface element

Because of the limited thickness of the mortar beds and mortar head joints, a linear finite element has been proposed, Fig. 2. If a local Cartesian base $\{O, x, y\}$

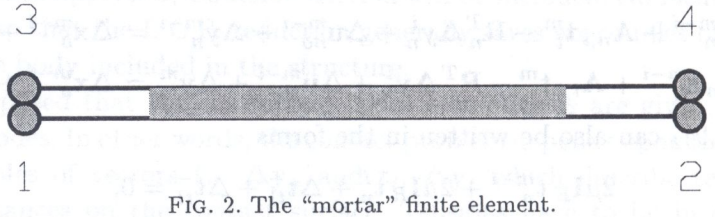

FIG. 2. The "mortar" finite element.

is chosen, O being the geometrical center and x the horizontal axis, the effective contact area will be defined by the edge points with coordinates, say x_i and x_f, where transition from contact to non-contact occurs. These points are taken as the extreme points of integration and remain undefined as parameters, so that the stiffness matrix will be referred only to the portion of the film being effectively in contact with the bricks (dashed area in Fig. 2). In other words, the stiffness matrix will be a function of the coordinates of the extreme points of contact.

In the plane case, the operators $\mathbf{D}$ and $\mathbf{C}$ in (2.1), (2.2) and (2.3) become

$$\mathbf{D} = \begin{bmatrix} \dfrac{\partial}{\partial x} & 0 \\ 0 & \dfrac{\partial}{\partial y} \\ \dfrac{\partial}{\partial y} & \dfrac{\partial}{\partial x} \end{bmatrix}, \tag{3.28}$$

$$
\begin{aligned}
\mathbf{C}_\sigma &= \frac{\mathbf{E}}{1-\nu^2}\begin{bmatrix} 1 & \nu & 0 \\ \nu & 1 & 0 \\ 0 & 0 & \dfrac{1-\nu}{2} \end{bmatrix}, \\
\mathbf{C}_\varepsilon &= \frac{\mathbf{E}}{(1+\nu)(1-2\nu)}\begin{bmatrix} 1-\nu & \nu & 0 \\ \nu & 1-\nu & 0 \\ 0 & 0 & \dfrac{1-2\nu}{2} \end{bmatrix},
\end{aligned}
\tag{3.29}
$$

where $\mathbf{C}_\sigma$ and $\mathbf{C}_\varepsilon$ are the constitutive matrices, respectively, in the plane stress and in the plane strain cases.

Considering a four-node element and the same linear shape functions for both displacements along x and y axis, the generic displacement vector $\mathbf{u}_f(\mathbf{x})$ takes the form

$$
\mathbf{u}_f(\mathbf{x}) = \begin{vmatrix} u_f \\ v_f \end{vmatrix} = \begin{vmatrix} \sum_{i=1}^{4} u_i \varphi_i(\mathbf{x}) \\ \sum_{i=1}^{4} v_i \varphi_i(\mathbf{x}) \end{vmatrix} = \begin{bmatrix} \varphi_1 & 0 & \varphi_2 & 0 & \varphi_3 & 0 & \varphi_4 & 0 \\ 0 & \varphi_1 & 0 & \varphi_2 & 0 & \varphi_3 & 0 & \varphi_4 \end{bmatrix} \begin{vmatrix} u_1 \\ v_1 \\ u_2 \\ v_2 \\ u_3 \\ v_3 \\ u_4 \\ v_4 \end{vmatrix}. \tag{3.30}
$$

In absolute notation:

$$
\mathbf{u}_f(\mathbf{x}) = \mathbf{\Phi}^t(\mathbf{x})\mathbf{u}. \tag{3.31}
$$

The stress and strain are

$$
\boldsymbol{\varepsilon} = \mathbf{D}\mathbf{\Phi}^t(\mathbf{x}) = \mathbf{B}\mathbf{u}, \qquad \sigma = \mathbf{C}\mathbf{B}\mathbf{u}. \tag{3.32}
$$

The stiffness matrix and the force vector are

$$
\mathbf{K}_{\Omega^c} = \int_{\Omega^c} \mathbf{B}^t\mathbf{C}\mathbf{B}\, d\Omega, \qquad \mathbf{f} = \int_{\Omega} \mathbf{\Phi}^t \mathbf{b}\, d\Omega. \tag{3.33}
$$

The film element is supposed to consist of a strip with the two surfaces at a relative distance t_y undergoing different displacements:

$$
\begin{aligned}
u_- &= u_{12} = \varphi^- u_1 + \varphi^+ u_2\,, \\
u_+ &= u_{34} = \varphi^- u_3 + \varphi^+ u_4\,, \\
v_- &= v_{12} = \varphi^- v_1 + \varphi^+ v_2\,, \\
v_+ &= v_{34} = \varphi^- v_3 + \varphi^+ u_4\,,
\end{aligned}
\tag{3.34}
$$

where

$$\varphi^- = \left[\frac{1}{2} - \frac{x}{l}\right], \qquad \varphi^+ = \left[\frac{1}{2} + \frac{x}{l}\right], \qquad -\frac{l}{2} \le x \le \frac{l}{2}. \tag{3.35}$$

The average variations of the displacements are:

$$\begin{aligned} \frac{\partial u_a}{\partial x} &= \frac{\partial}{\partial x}\left[\frac{u_+ + u_-}{2}\right], & \frac{\partial u_a}{\partial y} &= \frac{\triangle u}{t_y}, \\ \frac{\partial v_a}{\partial x} &= \frac{\partial}{\partial x}\left[\frac{v_+ + v_-}{2}\right], & \frac{\partial v_a}{\partial y} &= \frac{\triangle v}{t_y}, \end{aligned} \tag{3.36}$$

where $\triangle u = [u_+ - u_-]$ and $\triangle v = [v_+ - v_-]$. The deformation can be consequentely written as

$$\begin{aligned} \varepsilon_x &= \frac{\partial u_a}{\partial x} = \varphi^-_{,x}\left[\frac{u_1 + u_3}{2}\right] + \varphi^+_{,x}\left[\frac{u_2 + u_4}{2}\right], \\ \varepsilon_y &= \frac{\triangle v}{t_y} = \varphi^-\left[\frac{v_3 - v_1}{t_y}\right] + \varphi^+\left[\frac{v_4 - v_2}{t_y}\right], \\ \gamma_{xy} &= \frac{\partial u_a}{\partial y} + \frac{\partial v_a}{\partial x} = \varphi^-\left[\frac{u_3 - u_1}{t_y}\right] + \varphi^+\left[\frac{u_4 - u_2}{t_y}\right] \\ &\qquad + \varphi^-_{,x}\left[\frac{v_1 + v_3}{2}\right] + \varphi^+_{,x}\left[\frac{v_2 + v_4}{2}\right], \end{aligned} \tag{3.37}$$

where the matrix $\mathbf{B}$ becomes

$$\mathbf{B} = \begin{bmatrix} \frac{\varphi^-_{,x}}{2} & 0 & \frac{\varphi^+_{,x}}{2} & 0 & \frac{\varphi^-_{,x}}{2} & 0 & \frac{\varphi^+_{,x}}{2} & 0 \\ 0 & -\frac{\varphi^-}{t_y} & 0 & -\frac{\varphi^+}{t_y} & 0 & \frac{\varphi^-}{t_y} & 0 & \frac{\varphi^+}{t_y} \\ -\frac{\varphi^-}{t_y} & \frac{\varphi^-_{,x}}{2} & -\frac{\varphi^+}{t_y} & \frac{\varphi^+_{,x}}{2} & \frac{\varphi^-}{t_y} & \frac{\varphi^-_{,x}}{2} & \frac{\varphi^+}{t_y} & \frac{\varphi^+_{,x}}{2} \end{bmatrix}. \tag{3.38}$$

Finally the stiffness matrix will be

$$\mathbf{K}_{\Omega^c} = \int_{-t_z/2}^{t_z/2} dz \int_{-t_y/2}^{t_y/2} dy \int_{x_i}^{x_f} \mathbf{B}^t\mathbf{C}\mathbf{B}\, dx = t_z t_y \int_{x_i}^{x_f} \mathbf{B}^t\mathbf{C}\mathbf{B}\, dx. \tag{3.39}$$

A peculiarity of this finite element is that the stiffness matrix varies as a function of the contact area. In other words, the contact conditions are automatically satisfied by the global stiffness matrix $\mathbf{K}_{pf}$ in (3.17).

3.4. The nodal coordinates change method

Considering the mortar element shown in the previous section and trying to maximize the number of the bricks in the mesh, it becomes natural to assume for the bricks a four-node element.

Thus looking at the Fig. 3 it is obvious that, in order to connect any horizontal film to the nodal points of the bricks, changes in the nodal coordinates of each horizontal film are necessary.

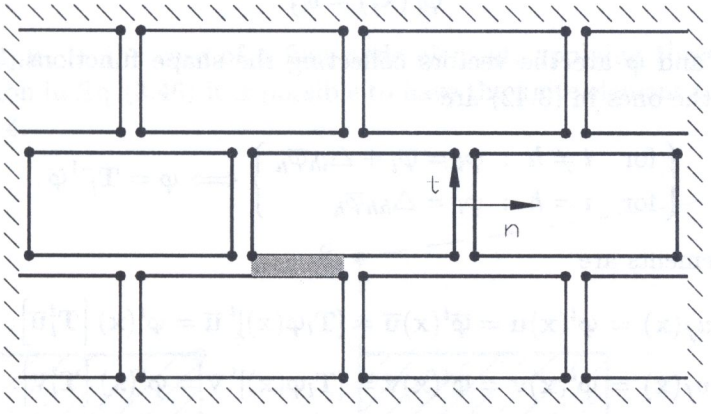

FIG. 3. Masonry discretization

In the literature it is well known how to change the topology of the entire element using a one-to-one mapping that changes all the coordinates of every point in the element, and consequentely the nodal points too. In this case, the problem is quite different because only changes of the coordinates of some nodal points are needed. All the other points are left unchanged. Due to author's knowledge, such procedure has not been presented in literature, thus it will be briefly introduced.

It is well known that the shape functions are orthonormal:

$$\varphi_i(\mathbf{x}_j) = \delta_{ij}\,, \tag{3.40}$$

where δ_{ij} is the Kronecker symbol. If a node, say the h-th node $\mathbf{x}_h$, is supposed to vary its coordinates in the space from $\mathbf{x}_h$ to $\overline{\mathbf{x}}_h$:

$$\overline{\mathbf{x}}_i \neq \mathbf{x}_i \quad \text{if} \quad i = h, \qquad \overline{\mathbf{x}}_i = \mathbf{x}_i \quad \text{if} \quad i \neq h,$$

Eq. (3.40) is lost

$$\varphi_i\,(\overline{\mathbf{x}}_j) = \triangle_{ij}\,. \tag{3.41}$$

Introducing the new shape functions $\overline{\varphi}_i$:

$$\left.\begin{array}{ll} \text{for} & i \neq h \ : \ \overline{\varphi}_i = \varphi_i - \dfrac{\triangle_{ih}}{\triangle_{hh}}\varphi_h \\ \text{for} & i = h \ : \ \overline{\varphi}_i = \dfrac{1}{\triangle_{hh}}\varphi_h \end{array}\right\} \Longleftrightarrow \overline{\boldsymbol{\varphi}} = \mathbf{T}_l \boldsymbol{\varphi}, \tag{3.42}$$

the orthonormal condition is soon recovered

$$\overline{\varphi}_i\left(\overline{\mathbf{x}}_j\right) = \delta_{ij}\,. \tag{3.43}$$

In (3.43) $\overline{\boldsymbol{\varphi}}$ and $\boldsymbol{\varphi}$ are the vectors collecting the shape functions. The inverse relations of the ones in (3.42) are

$$\left.\begin{array}{ll} \text{for} & i \neq h \ : \ \varphi_i = \overline{\varphi}_i + \triangle_{ih}\overline{\varphi}_h \\ \text{for} & i = h \ : \ \varphi_i = \triangle_{hh}\overline{\varphi}_h \end{array}\right\} \Longleftrightarrow \boldsymbol{\varphi} = \mathbf{T}_l^{-1}\overline{\boldsymbol{\varphi}}\,. \tag{3.44}$$

The displacements are

$$\begin{aligned} u_f(\mathbf{x}) &= \boldsymbol{\varphi}^t(\mathbf{x})\mathbf{u} = \overline{\boldsymbol{\varphi}}^t(\mathbf{x})\overline{\mathbf{u}} = \left[\mathbf{T}_l\boldsymbol{\varphi}(\mathbf{x})\right]^t\overline{\mathbf{u}} = \boldsymbol{\varphi}^t(\mathbf{x})\left[\mathbf{T}_l^t\overline{\mathbf{u}}\right], \\ v_f(\mathbf{x}) &= \boldsymbol{\varphi}^t(\mathbf{x})\mathbf{v} = \overline{\boldsymbol{\varphi}}^t(\mathbf{x})\overline{\mathbf{v}} = \left[\mathbf{T}_l\boldsymbol{\varphi}(\mathbf{x})\right]^t\overline{\mathbf{v}} = \boldsymbol{\varphi}^t(\mathbf{x})\left[\mathbf{T}_l^t\overline{\mathbf{v}}\right]. \end{aligned} \tag{3.45}$$

Because of the inner products in (3.45), the change in the shape functions from $\boldsymbol{\varphi}(\mathbf{x})$ to $\overline{\boldsymbol{\varphi}}(\mathbf{x})$ by $\mathbf{T}_l$ has the same effect as a change of bases from $\mathbf{u}$ to $\overline{\mathbf{u}}$ given by the transpose $\mathbf{T}_l^t$. Collecting the two equations (3.45), the displacement field $\mathbf{u}_f(\mathbf{x}) = (u_f(\mathbf{x}), v_f(\mathbf{x}))^t$ becomes

$$\mathbf{u}_f(\mathbf{x}) = \boldsymbol{\Phi}^t(\mathbf{x})\mathbf{u} = \left[\mathbf{T}_q\boldsymbol{\Phi}(\mathbf{x})\right]^t\overline{\mathbf{u}} = \boldsymbol{\Phi}^t(\mathbf{x})\left[\mathbf{T}_q^t\overline{\mathbf{u}}\right]. \tag{3.46}$$

It is now clear that, as said before, changing the $\boldsymbol{\varphi}$ bases by $\mathbf{T}_q$ is equivalent to the change of the nodal bases by $\mathbf{T}_q^t$. If for example, a four-node element is considered and the second node assumes new coordinates, following the numbers: $u_1, \ldots, u_4, v_1, \ldots, v_4$, $\mathbf{T}_q$ has the form

$$\mathbf{T}_q = \begin{bmatrix} \mathbf{T}_l & \mathbf{0} \\ \mathbf{0} & \mathbf{T}_l \end{bmatrix}, \tag{3.47}$$

where

$$\mathbf{T}_l = \begin{bmatrix} 1 & \triangle_{12} & 0 & 0 \\ 0 & \triangle_{22} & 0 & 0 \\ 0 & \triangle_{32} & 1 & 0 \\ 0 & \triangle_{42} & 0 & 1 \end{bmatrix}, \qquad \mathbf{T}_l^{-1} = \begin{bmatrix} 1 & -\triangle_{12}/\triangle_{22} & 0 & 0 \\ 0 & 1/\triangle_{22} & 0 & 0 \\ 0 & -\triangle_{32}/\triangle_{22} & 1 & 0 \\ 0 & -\triangle_{42}/\triangle_{22} & 0 & 1 \end{bmatrix}. \tag{3.48}$$

Observing the second columns in (3.48) it is easy to recognize whether $\mathbf{T}_l$ is invertible or not. If $\triangle_{22}$ or its inverse are equal to zero, the second columns are linear combinations of the remaining ones. The physical meaning is that the new node cannot coincide with other nodes, ($\triangle_{22} \to 0$), neither it can be very far from the previous position, ($\triangle_{22} \to \pm\infty$). Therefore:

$$\left\{ \begin{array}{c} \triangle_{22} \neq 0 \\ 1/\triangle_{22} \neq 0 \end{array} \right\} \Longleftrightarrow \mathbf{T} \quad \text{is invertible.} \tag{3.49}$$

For example, in the case of a four-node element, applying three times the transformation in Eq. (3.46) it is possible to have the finite element shown at the right in Fig. 4.

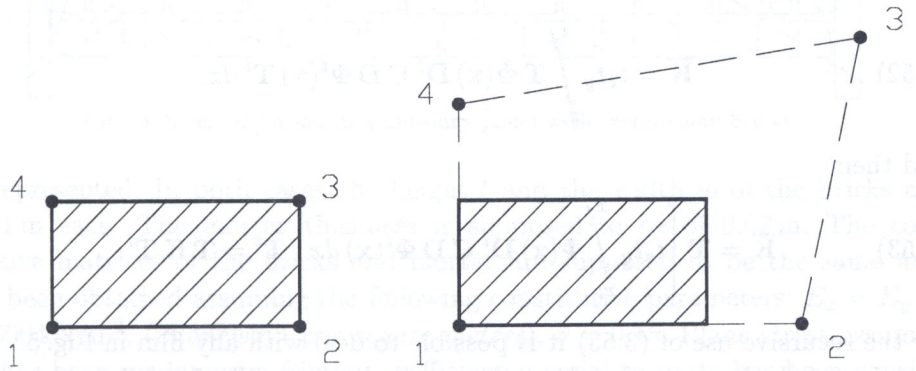

FIG. 4. Changes in the nodal coordinates of a 4-node element.

Obviously, if the transformation is applied, for example, to an isoparametric element, also the effective area of the element, the dashed area in the figure, can vary its shape.

In the case of the mortar films (Fig. 5), although four linear shape functions are needed, coupling occurs only beetween the two shape functions lying on the same side.

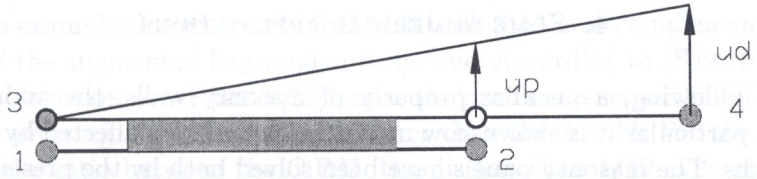

FIG. 5. Change of coordinates of the 4-th node.

For this reason, the transformation matrix $\mathbf{T}_q$, for a change of coordinate occurring in the fourth node but following the node numeration: u_1, v_1, ..., u_4,

v_4, has the form:

$$\mathbf{T}_q = \begin{bmatrix} \mathbf{T}_l & \mathbf{0} \\ \mathbf{0} & \mathbf{I} \end{bmatrix}, \qquad \mathbf{T}_l = \begin{bmatrix} 1 & 0 & 0 & 0 \\ 0 & 1 & 0 & 0 \\ \beta & 0 & \alpha & 0 \\ 0 & \beta & 0 & \alpha \end{bmatrix}, \tag{3.50}$$

where

$$\alpha = \frac{l}{l + \triangle l}, \qquad \beta = \frac{\triangle l}{l + \triangle l}. \tag{3.51}$$

In (3.51) l is the length of the film and $\triangle l$ is the variation of the coordinates: $\triangle l = (\overline{x}_n - x_n)$. To conclude, the new stiffness matrix is

$$\overline{\mathbf{K}} = t_z t_y \int_{x_i}^{x_f} \mathbf{T}\, \mathbf{\Phi}(\mathbf{x})\, \mathbf{D}^t\, \mathbf{C}\, \mathbf{D}\, \mathbf{\Phi}^t(\mathbf{x})\, \mathbf{T}^t\, dx, \tag{3.52}$$

and then

$$\overline{\mathbf{K}} = \mathbf{T} \left[t_z t_y \int_{x_i}^{x_f} \mathbf{\Phi}(\mathbf{x})\, \mathbf{D}^t\, \mathbf{C}\, \mathbf{D}\, \mathbf{\Phi}^t(\mathbf{x})\, dx \right] \mathbf{T}^t = \mathbf{T}\, \mathbf{K}\, \mathbf{T}^t. \tag{3.53}$$

By the recursive use of (3.53) it is possible to deal with any film in Fig. 5.

• In conclusion, starting from the mesh shown in Fig. 5, a general method for moving the nodes, without changing the shape and the properties of every finite element, has been recovered. It is important to stress that this procedure, by means of (3.53), makes it also possible to obtain the effective stiffness matrix bypassing (3.39). It is enough to consider a master element, to calculate the stiffness matrix of a film element of a length equal to $|x_f - x_i|$, and then to apply the changes to the nodal coordinates.

4. Some numerical applications

In the following, a peculiar property of masonry walls, the arch effect, is shown. In particular it is shown how much this property is affected by the shape of the bricks. The masonry panels have been solved both by the presented linear complementarity formulation and by the augmented Lagrangian method so that their performances can be compared.

In Figs. 6 and 7, two masonry panels with the same overall sizes but made of bricks of two different lengths, rectangular ($l = 0.20\,\mathrm{m}$) and square ($l = 0.10\,\mathrm{m}$),

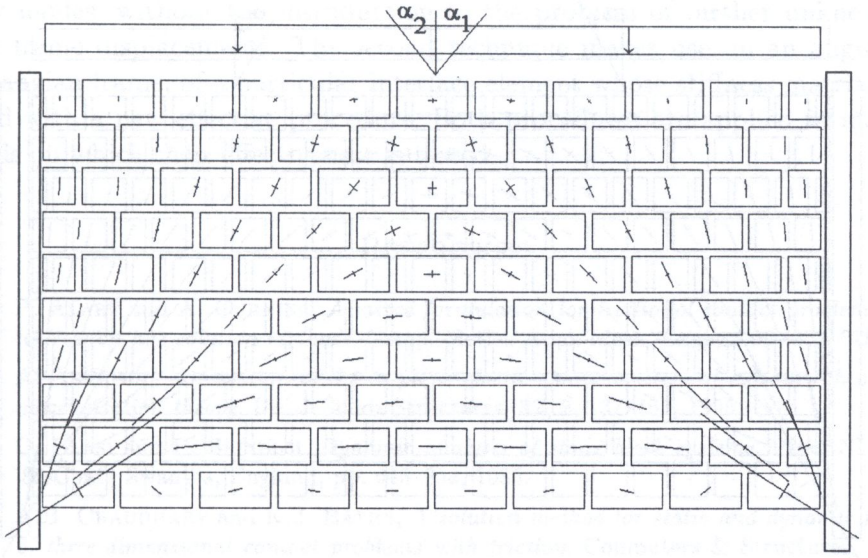

FIG. 6. Stress diffusion in a masonry panel with *rectangular* bricks.

are represented. In both cases the height l and the width w of the bricks are of 0.1 m each. The mortar thickness is supposed to be of 0.02 m. The constitutive matrices of the bricks and mortar are supposed to be the same and have been obtained assuming the following constitutive parameters: $E_x = E_y = 100.000\,\mathrm{kN/m^2}$, (*kilonewton* per *square meters*), $\nu = 0.15$. Plane stress assumption has been made and a friction coefficient μ equal to unity has been considered. Both panels have on the top a vertical distributed load of $10\,\mathrm{kN/m^2}$ and are thought to be between two indefinitely rigid vertical walls in unilateral contact with Coulomb friction ($\mu = 1$). The principal stresses are reported. Though the arch effect is very clear in both the cases, it can be noted that the principal stresses try to follow two different lines very close to those which, starting from the lower corners of the panel, make the angles $\alpha_1, \alpha_2 = \pm \arctan(l/2h)$ with the vertical axis y. This seems to be the natural consequence of the actual texture of the bricks.

The two examples have been studied with both the linear complementarity approach and the augmented Lagrangian technique. According to (STAVROULAKIS, PANAGIOTOPOULOS, AL-FAHED [27]), once the problem is set in the L.C.P. form, the Lemke pivoting algorithm is much faster than the A.L.M. For the following examples, the ratio between the C.P.U. time is less than 1/10. The real limitation of the L.C.P. reduction comes from the size of the problem. Starting from the same memory available, while L.C.P. formulation with pivoting needs a full double matrix of order $n \times 2n$, the A.L.M. can employ a banded matrix of order $n \times sb$ where sb is one half the band of the problem.

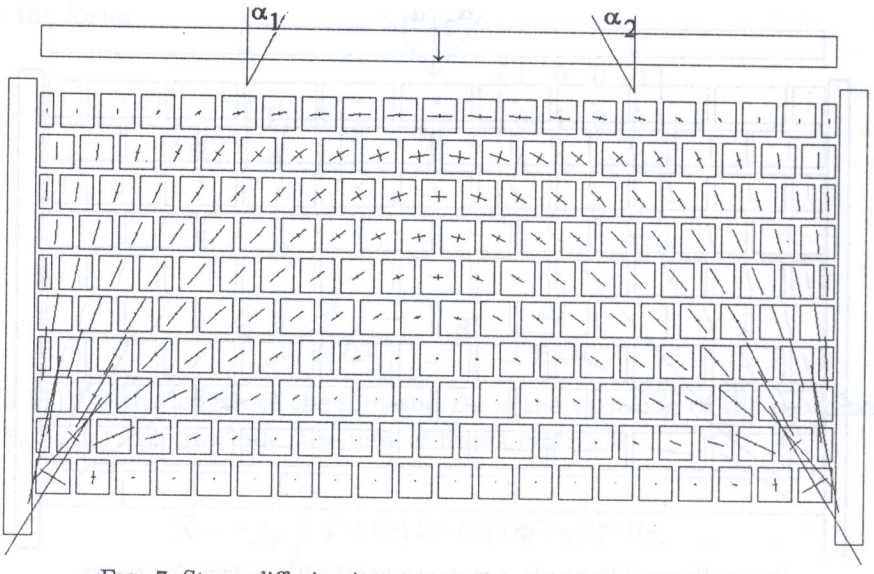

FIG. 7. Stress diffusion in a masonry panel with *square* bricks.

For example, the square wall in Fig. 7 is reduced to an L.C.P. approximately of order 1600×3200, while using the A.L.M. it is "only" of order 1600×160. It must be said that to obtain a good approximation (1/10.000 of unbalanced forces), generally 15 – 30 iterations, with stiffness matrix updating, are needed but, as a general feature, problems of much larger size can be analysed. Further, although the L.C.P. formulation is formally very actractive because it deals with both the parameters and their complementarity counterpart, the L.C.P reduction takes time to be made and the procedure is not so immediate as the A.L.M. which is also very simple to implement in a code. In authors' opinion, in order to be competitive in memory saving, an iterative L.C.P. procedure should be used. It is convenient for this purpose to change the problem in order to recover a minimum principle, as it was done in (STAVROULAKIS, PANAGIOTOPOULOS, AL-FAHED [27]) where "soft" elastic constraints have been introduced to avoid the free body modes. This approach allows the problem be solved by the usual iterative techniques (COTTLE, PANG, STONE [5]).

5. CONCLUSIONS

In the paper, two different numerical procedures for the solution of the two-dimensional frictional contact problems with Coulomb's law of friction are presented. The first procedure reduces the contact problem to a new linear complementarity problem which shows the interesting feature of dealing with rigid

body modes, without the introduction to the problem of further unknowns as local frame displacements. The second technique makes use, in an augmented Lagrangian frame, of a particular interface element whose stiffness matrix is updated with a new effective procedure. Both procedures are applied to masonry panels on which their effectiveness is tested.

REFERENCES

1. P. ALART and A. CURNIER, *A mixed formulation for frictional contact problems prone to Newton like solution methods*, Comp. Meths. Appl. Mech. Engng., **92**, 353–375, 1991.
2. A. ANTHOINE, *Derivation of the in-plane elastic characteristics of masonry through homogeneization theory*, Int. J. Solids Structures, **32**, 2, 137–163, 1995.
3. C. BLASI and P. SPINELLI, *Dynamic analysis of stone block systems*, Proc. NUMETA '85 Conf., Swansea, England, pp. 645–652, 1985.
4. A.B. CHAUDHARY and K.J. BATHE, *A solution method for static and dynamic analysis of three-dimensional contact problems with friction*, Computers & Structures, No. 24, pp. 853–873, 1986.
5. R.W. COTTLE, J.S. PANG and R.E. STONE, *The linear complementarity problem*, Academic Press, 1992.
6. G. DEL PIERO, *Recent developments in the mechanics of materials which do not support tension*, Proc. Int. Colloquium on Free Boundary Problems, Irsee, 1987.
7. G. DEL PIERO, *Constitutive equation and compability of the external loads for linear elastic masonry-like materials*, Meccanica, **24**, 150–162, 1989.
8. G. DEL PIERO, *Resolution methods for framed structures with unilateral constraints* [in Italian], IMTA, Institute of Theoretical and Applied Mechanics, University of Udine, Italy 1990.
9. G. DEL PIERO, *Shock dynamics for a rigid block over a rigid foundation*, Proc. Contact Mechanics International Symposium, Lausanne, Suisse 1992.
10. G. DE SAXCE and Z.Q. FENG, *New inequality and functional for contact with friction: the implicit standard material approach*, Mech. Struct. & Mach., **19**, 3, 301–325, 1991.
11. A. ERCOLANO, *Numerical simulations of superimposed block structures in finite displacements*, The Sixth North American Masonry Conference, Philadelphia, U.S.A. 1993.
12. A. ERCOLANO, *On a Lagrangian approach to the dynamics of superimposed block structures*, 2nd International Conference On Computational Structures Technology, Athens, Greece 1994.
13. V. FRANCIOSI, *L'attrito nel calcolo a rottura delle murature*, Giornale del Genio Civile, 7.8.9, 1980.
14. M. GIAQUINTA and E. GIUSTI, *Researches on the equilibrium of masonry structures*, Arch. Rational Mech. Analysis, **68**, 359–392, 1985.
15. J. HEYMAN, *The stone skeleton*, Int. J. Solids Struct., **2**, 1966.
16. Y. ISHIYAMA, *Motions of rigid bodies and criteria for overturning by earthquake exitations*, Earthquake Engng. and Struc. Dynamics, No. 10, pp. 635–650, 1982.

17. LEE SEOK-SOON, *A computational method for frictional contact problem using finite element method*, Inter. J. Num. Methods Engng., **37**, 217–228, 1994.

18. R.K. LIVESLEY, *Limit analysis of structures formed from rigid blocks*, Int. J. Num. Meth. Engng., **12**, 1853–1871, 1978.

19. R. LUCIANO and E. SACCO, *Homogenization technique and damage model for old masonry material* [to appear on Int. J. Solids Structures].

20. N. KIKUCHI and J.T. ODEN, *Contact problems in elasticity*, SIAM, Philadelphia 1988.

21. A. KLARBRING, *Contact problems with friction. Thesis*, Linköping Institute of Technology, Linköping, Sweden 1984.

22. A. KLARBRING, *Mathematical programming and augmented Lagrangian methods for frictional contact problems*, Contact Mechanics Int. Symposium, Switzerland 1992.

23. G.N. PANDE, J.X. LIANG and J. MIDDLETON, *Equivalent elastic moduli for brick masonry*, Comput. Geotechnics, **8**, 243–265, 1989.

24. S. PIETRUSZCZAK and X. NIU, *A mathematical description of macroscopic behaviour of brick masonry*, Int. J. Solids Structures, **29**, 5, 531–546, 1991.

25. G. ROMANO and M. ROMANO, *Sulla soluzione di problemi strutturali in presenza di legami costitutivi unilateri*, Rend. Acc. Naz. dei Lincei, Classe Scienze Fisiche, Matematiche e Naturali, Serie VIII, **67**, 1979.

26. J.C. SIMO and T.A. LAURSEN, *An augmented Lagrangian treatment of contact problems involving friction*, Computers & Structures, **42**, 97–116, 1992.

27. G.E. STAVROULAKIS, P.D. PANAGIOTOPOULOS and A.M. AL-FAHED, *On the rigid body displacements and rotations in unilateral contact problems and applications*, Computers & Structures, **40**, 3, 599–614, 1991.

28. C.S. YIM, A.K. CHOPRA and J. PENZIEN, *Rocking response of rigid blocks to earthquakes*, Earthquake Engng. and Struct. Dynamics, **8**, 6, pp. 565–587, 1989.

DEPARTMENT OF STRUCTURAL MECHANICS,
UNIVERSITY OF BASILICATA, POTENZA, ITALY

and

DEPARTMENT OF INDUSTRIAL ENGINEERING,
UNIVERSITY OF CASSINO, CASSINO, ITALY.

Received February 28, 1997; new version July 2, 1997.